FusedAR: Energy-Positive Human Activity Recognition Using Kinetic and Solar Signal Fusion

Muhammad Moid Sandhu, *Member, IEEE*, Sara Khalifa, *Member, IEEE*, Kai Geissdoerfer, Raja Jurdak, *Senior Member, IEEE*, Marius Portmann, *Member, IEEE*, and Brano Kusy, *Member, IEEE*

***Abstract*—Today's wearable Internet of Things (IoT) devices, which have numerous practical applications, suffer from the limited lifetime of batteries due to the high power consumption of conventional inertial activity sensors. Recently, kinetic energy harvesters have been employed as a source of energy as well as context information to replace conventional activity sensors. However, the harvested power from human movements using miniaturized kinetic transducers may not be sufficient to enable a perpetual and self-powered activity recognition system. In this article, we propose a novel mechanism of fused signal-based human activity recognition (FusedAR), which employs miniaturized wearable solar and kinetic energy harvesters simultaneously as an energy source as well as an activity sensor. As human activities engender distinct movement patterns and interact and interfere with the ambient light differently, the kinetic and solar energy harvesting (SEH) signals incorporate unique information about the underlying activities while generating sufficient power. After detailed experiments, we find that the FusedAR, which employs both solar and kinetic energy signals, achieves superior activity recognition performance by up to 10%, particularly in outdoor and night-time contexts, and can recognize not only activities but also contexts, compared with the individual energy harvesting signals. Furthermore, our analysis demonstrates that FusedAR, in addition to significant energy generation, consumes up to 22% less power than the highly optimized conventional three-axis accelerometer-based mechanisms, achieving *energy-positive* human activity recognition (HAR) leading toward perpetual, uninterrupted, and autonomous operation of wearable IoT devices.**

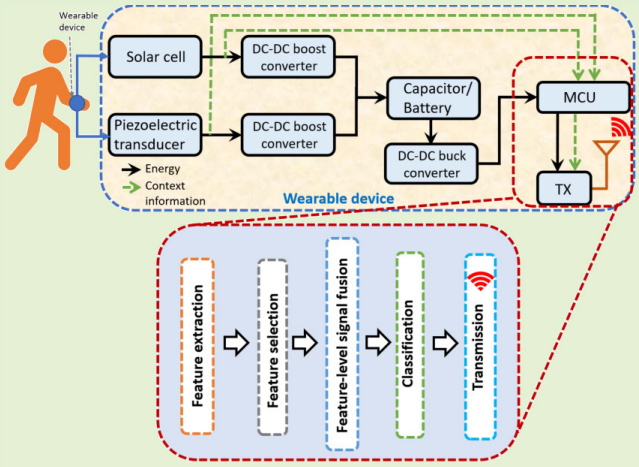

***Index Terms*— Context detection, energy harvesting, energy-positive sensors, fused signals, human activity recognition (HAR), Internet of Things (IoT), kinetic, solar, wearables.**

I. Introduction

THE proliferation of mobile devices, ubiquitous internet, and cloud computing has triggered a new era of Internet of Things (IoT), which allows interaction between everyday objects to make smart decisions. Wearable IoT devices are becoming increasingly popular as technology advances, with an estimated market value of U.S. $265.4 billion by 2026 [1]. There are various commercially available wearable products, such as Fitbit [2], Garmin [3], and Apple watch [4], which have a wide range of applications in our daily lives, including activity monitoring, healthcare, fitness tracking, and transportation route planning [5]. However, due to the low energy storage capacity of current wearable devices' batteries, their lifetime is limited, restricting their adoption and widespread deployment [5]. Energy harvesters, which transform ambient energy in the environment, such as solar, kinetic, thermal, and radio frequency waves into electrical energy to power these wearable IoT devices [6], are a possible alternative. Energy harvesters can also be used as activity/context sensors

Manuscript received 14 March 2023; accepted 15 April 2023. Date of publication 25 April 2023; date of current version 31 May 2023. This work was supported in part by The University of Queensland and in part by the Data 61 CSIRO, Australia. This is an expanded paper from the IEEE International Conference on Pervasive Computing and Communications (PerCom) 2021. The associate editor coordinating the review of this article and approving it for publication was Dr. Qammer H. Abbasi. *(Corresponding author: Muhammad Moid Sandhu.)*

This work involved human subjects in its research. Approval of all ethical and experimental procedures and protocols was granted by the Ethics Committee, CSIRO, and The University of Queensland, under Approval No. 106/19 and 2019001916/106/19, respectively.

Please see the Acknowledgment section of this article for the author affiliations.

Digital Object Identifier 10.1109/JSEN.2023.3268687

TABLE I
COMPARISON WITH THE STATE OF THE ART

Article - Year	Sensor		Signal fusion	Energy harvesting	Powered load	Context (indoors/outdoors)	Application
	KEH	SEH					
[8], [9] - 2017	✓	×	×	×	×	Indoors	Human activity recognition
[10], [11] - 2019	×	✓	×	×	×	Indoors	Hand gesture recognition
[12] - 2019	✓	✓	×	×	×	Indoors	Place recognition
[13] - 2020	✓	×	×	✓	×	Indoors	Human activity recognition
[14] - 2020	✓	×	×	✓	✓	Outdoors	Transport mode detection
[15] - 2021	×	✓	×	✓	✓	Indoors	Human activity recognition
Proposed - 2023	✓	✓	✓	✓	✓	Both	Human activity recognition

to replace traditional power-hungry inertial sensors, such as accelerometers and magnetometers [7], because the pattern of the energy harvesting signal correlates with the underlying physical motion and activity.

A. Background

Following this intuition, Khalifa et al. [8] show that the energy harvesting signal from a wearable kinetic energy harvesting (KEH) transducer varies in line with the underlying human movements and, thus, encodes distinct context information about the corresponding activity, demonstrating the potential of KEH-based activity recognition (KEHAR) as a proxy for conventional accelerometer-based activity recognition (AccAR) [16]. Moving one step further, Ma et al. [17] suggest that KEH can be employed for both sensing and energy harvesting simultaneously, while Sandhu et al. [14] demonstrate that KEH can support energy-positive signal acquisition, in which the harvested energy surpasses the energy required for acquiring the activity signal in human activity recognition (HAR) applications. This enables applications in which sensor data are logged locally on the embedded device and then manually uploaded for offline analysis after deployment. However, for users to receive real-time feedback on their activities, the harvested energy must be able to power not only on-device signal acquisition but also activity classification and transmission. Unfortunately, the harvested power from a tiny, single, untuned, and wearable-sized KEH transducer may not be sufficient to power all components of an end-to-end HAR system [14], [18].

B. Objective

Our main objective in this article is to implement end-to-end *energy-positive* HAR, where the harvested energy exceeds the energy required to acquire the activity signal, classify the activity, and wirelessly transmit the inferred activity class. A promising approach is to employ solar (photovoltaic) cells to harvest energy from the abundantly available ambient light. Previous works [19], [20] show that solar energy harvesting (SEH) offers higher power density, energy conversion efficiency, and robustness than piezoelectric-based KEH transducer, making SEH a favorable source to power IoT sensor nodes. In addition, as illustrated in Table I, solar cells have also been used previously for recognizing different types of hand gestures [10], [11] and room-level localization [12] in indoor settings, showing their potential as a proxy for activity sensors. Nevertheless, SEH has either been used as an energy source or as an activity sensor separately. Furthermore, to the best of our knowledge, the use of wearable solar cells to recognize human physical activities in HAR applications remains largely uninvestigated. Although our previous work [15] explores solar cell as a context/activity sensor, it does not study the performance of solar cell in diverse lighting conditions, such as at night and in various environments (indoor and outdoor).

KEH and SEH have their own advantages and limitations in generating energy and detecting the human activity. For example, KEH may not harvest sufficient energy during static activities (e.g., sitting and standing) to power the wearable device. In addition, due to weak energy harvesting signal, it is strenuous to differentiate between static activities using KEH signal. On the other hand, SEH is unable to generate sufficient energy at night and during low-light conditions, to perpetually power the wearable device. Therefore, this article proposes the fusion of both SEH and KEH signal to overcome their limitations and complement individual energy harvesting transducers. In addition, fusing the signals from solar and kinetic energy harvesters may offer higher HAR performance as well as higher harvested power. Table I clearly shows that previous works do not explore kinetic and solar signal fusion while using the harvested energy to power a dynamic load. In addition, previous works shown in Table I do not explore the implementation of end-to-end HAR classification pipeline using only the harvested energy from the transducers.

C. Contribution

In this article, we propose fused signal-based HAR (FusedAR), which employs both solar and kinetic energy harvesters simultaneously as sensors for activity recognition as well as sources of energy, as depicted in Fig. 1. The output harvesting signals from both transducers embed unique traces of the underlying context, because human activities interact and interfere with the ambient light differently and generate distinct vibration patterns. We empirically and extensively evaluate FusedAR using extended (real world)

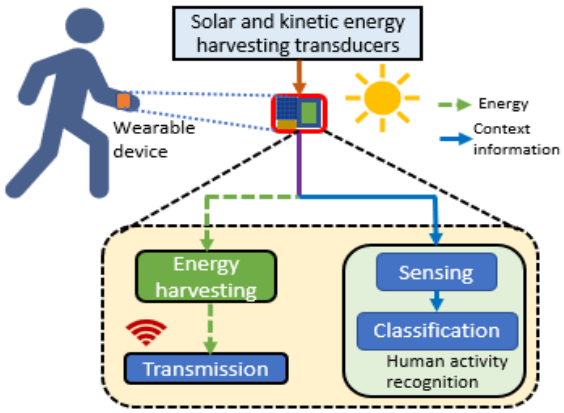

Fig. 1. Employing solar and KEH transducers for activity recognition as well as to power the wearable sensor node simultaneously, leading toward end-to-end *energy-positive* HAR.

datasets (indoors/outdoors and day/night) collected from 40 participants performing five common human activities in indoor and outdoor environments. We have presented the initial evaluation of solar-based human activity recognition (SolAR) in [15], whereas in this article, we rigorously evaluate SolAR in diverse lighting conditions (day/night) and discover that it can recognize activities not only during day times but also during night times when the ambient light is significantly limited. We implement the HAR classification algorithm on an ultralow-power micro-controller unit (MCU) to find that FusedAR harvests sufficient power to run the end-to-end HAR algorithm (including feature extraction, classification, and activity transmission) and, thus, ensures *energy-positive* HAR. Finally, we evaluate our proposed mechanism, using a metric of HAR power ratio (suitable for energy harvesting-based sensors), which is the ratio of harvested power and required power for implementing the HAR algorithm (see Section V-C). In the following, the major contributions of this article are summarized.

1) We propose FusedAR using both solar and KEH signals to enhance the HAR accuracy, showing that it improves HAR performance by up to 10% compared with the use of individual (solar or kinetic) energy harvesting signal.
2) We empirically evaluate FusedAR and SolAR using real-world enhanced datasets (collected from indoors/outdoors and day/night environments) and compare their performance with state-of-the-art methods, including KEHAR and conventional AccAR, demonstrating the potential of SolAR and FusedAR for accurate and reliable HAR.
3) Our experiments reveal that FusedAR and SolAR reduce power consumption by up to 22% compared with conventional AccAR and offer at least one order of magnitude higher harvested power compared with recently proposed KEHAR, delivering end-to-end *energy-positive* real-time HAR.

The remainder of this article is organized as follows. Section II provides the literature review and motivation, and Section III describes our proposed FusedAR architecture along with the implementation process. We evaluate FusedAR in Section IV and discuss the novel mechanism of end-to-end energy-positive HAR in Section V. Finally, we conclude this article and discuss the future directions in Section VII.

II. Literature Review and Motivation

This section describes previous wearable-based HAR mechanisms as well as the motivation behind this work.

A. Accelerometer-Based HAR

Previous research studies have shown that wearable IoT devices, based on inertial sensors, such as accelerometers and magnetometers [5], can be attached to different parts of the human body to achieve reliable HAR. These wearable devices have numerous practical applications, including health/fitness monitoring, activity detection, and tracking and localization [21]. Smarr et al. [22] and Ates et al. [23] propose that wearable devices, which monitor human physiological parameters, can be employed for the early recognition of asymptomatic and presymptomatic cases of COVID-19. In another work [24], a wrist wearable device is designed to detect the obstacles for providing independent mobility to visually impaired people. Sztyler et al. [25] employ a wearable device for HAR and suggest that it offers best results when placed on the waist. The major bottleneck of these wearable devices is their limited lifetime, which hinders their widespread adoption [8] and pervasive deployment. Although battery technology is evolving over time, their limited lifetime is still one of the biggest impediments to advancing wearable technology [5]. This opens the door to explore energy harvesting sources as viable alternatives for charging the batteries, which can ultimately result in the uninterrupted and autonomous operation of wearable IoT sensing devices.

B. KEH-Based HAR

Recently, KEH transducers have been used as an energy-efficient activity sensor. Khalifa et al. [8] suggest that the harvesting signal from a KEH transducer can be used for HAR to reduce the energy consumption compared with the conventional inertial sensors and to allow for perpetual operation of the wearable IoT device. Lan et al. [26] store the kinetic harvested energy in a capacitor and use the capacitor voltage signal for activity recognition. KEH transducers have also been used for monitoring food intake [27], recognizing transport modes [28], and generating security key for wearables [29]. In order to increase the energy generated from KEH, Ma et al. [17] employ two separate transducers in a shoe and use the harvesting signal for gait recognition. On the other hand, Sandhu et al. [14] employ a single KEH transducer simultaneously to harvest energy and to recognize the daily activities, and coin the term of *energy-positive* signal acquisition. However, the harvested energy from human movements/vibrations is not enough to ensure the autonomous operation of wearable devices [14], which led to exploring alternate HAR mechanisms harvesting sufficient energy to ensure the perpetual and autonomous operation of wearable IoT devices.

TABLE II
SEH AND KEH PROPERTIES [19], [20]

Property	Photovoltaic	Piezoelectric
Power density [$\mu W/cm^2$]	$10\,\mu W$ to $15\,mW$	upto $330\,\mu W$
Energy conversion efficiency	up to 40%	up to 30%
Robustness	High	Low

C. SEH-Based HAR

SEH offers significant benefits in terms of power density, energy conversion efficiency, and robustness compared with KEH, as shown in Table II. Therefore, SEH can be considered as an attractive source to power IoT sensor nodes [30]. Solar cells have been also used as a proxy for recognizing hand gestures and room-level localization. Ma et al. [10], [11] use a solar cell to identify and recognize various hand gestures under a lamp light in an indoor environment. As the movement of the hand obstructs the light falling on the solar surface, the resulting harvesting signal contains information about the gestures performed. On the other hand, Umetsu et al. [12] employ multisource energy harvesters, including solar and kinetic, for place recognition in an indoor environment. However, these works [10], [11], [12] employ SEH merely as a context sensor without extracting energy simultaneously and, thus, do not fully reap the benefits of the energy harvesters. Furthermore, to the best of our knowledge, the use of solar cells to recognize human physical activities in HAR applications remains largely uninvestigated. In an initial study called SolAR [15], we show the potential use of solar cell as a simultaneous source of energy and context information for recognizing human physical activities. In this article (see Section IV), we provide an extensive evaluation of SolAR in diverse lighting conditions and using a large cohort of participants.

D. Motivation

Previous studies [8], [14] have shown that KEH can be employed as a simultaneous source of energy and context information. However, the limited harvested energy from a miniaturized KEH transducer is not sufficient to perpetually run the wearable IoT device [14]. Table II shows that SEH offers higher power density and, thus, can offer higher harvested energy compared to a KEH transducer. Sandhu et al. [15] proposed the use of SEH as a simultaneous source of energy and context information and showed that SEH offers better results in terms of harvested energy and activity recognition compared with KEH-based sensing. However, SEHs are unable to harvest sufficient power during night (and low-light conditions) [15] and, thus, cannot capture activities performed in low-light conditions and in dark environments. Table I shows that previous works use either KEH or SEH for activity/context recognition without using the harvested energy to power a dynamic load. Although Umetsu et al. [12] employ both KEH and SEH transducers, they neither use fusion nor harvest the energy to power a real-world dynamic load.

Our article is motivated by the fact that both kinetic and solar energy harvesters can be employed simultaneously for activity recognition and energy harvesting. Due to the varying movements and unique interactions with the ambient light, as depicted in Fig. 2, both KEH and SEH signals can be fused to obtain high harvested energy and enhanced sensing performance. Table I shows the novelty of our work compared with previous works in terms of sensing using KEH and SEH signal fusion and simultaneous energy harvesting to power a dynamic load. Note that both KEH and SEH transducers embed the context information differently, i.e., from the changing vibration signals and the varying light intensity, respectively. As activity signals from both transducers complement each other, the resultant high-fidelity fused signal can offer fine-grained information about the underlying activities. In addition, energy can be harvested even during static activities (from SEH) and low-light conditions (from KEH), resulting in near-perpetual operation of wearable IoT devices.

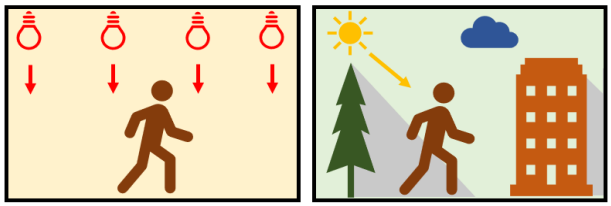

Fig. 2. Difference of light sources, shadowing and variation in light intensity in (a) indoors and (b) outdoors.

III. FUSEDAR: HAR USING SOLAR AND KINETIC ENERGY SIGNALS

We describe the architecture of our proposed fusion-based activity recognition (FusedAR) system in Section III-A and the implementation specific details in Sections III-B–III-D.

A. Architecture of FusedAR

We employ a wearable kinetic energy harvester and a solar cell simultaneously as activity sensors for activity recognition and energy sources to run the system load for the self-powered operation of wearable IoT sensing devices. Fig. 3 shows the architecture of our proposed fusion-based activity recognition (FusedAR) model. We employ an ultralow power dc–dc boost converter with maximum power point tracking for both transducers, to optimize the harvested power [31] as well as to decouple the harvesting signal from the energy storage and load behavior [14]. The dc–dc buck converter provides a constant supply voltage when the voltage of the capacitor (or battery) exceeds a configurable threshold. The combined stored harvested energy (in a capacitor/battery) is used to power the system load using a converter to match the capacitor voltage with the system specifications. Using the proposed architecture, the context information is only embedded in the harvesting current signal, because the converter regulates the transducer voltage according to the maximum power point tracking algorithm. We employ an MCU to acquire and collect the harvesting current signals from both transducers and to recognize the underlying activity using a machine learning model, as portrayed in Fig. 3.

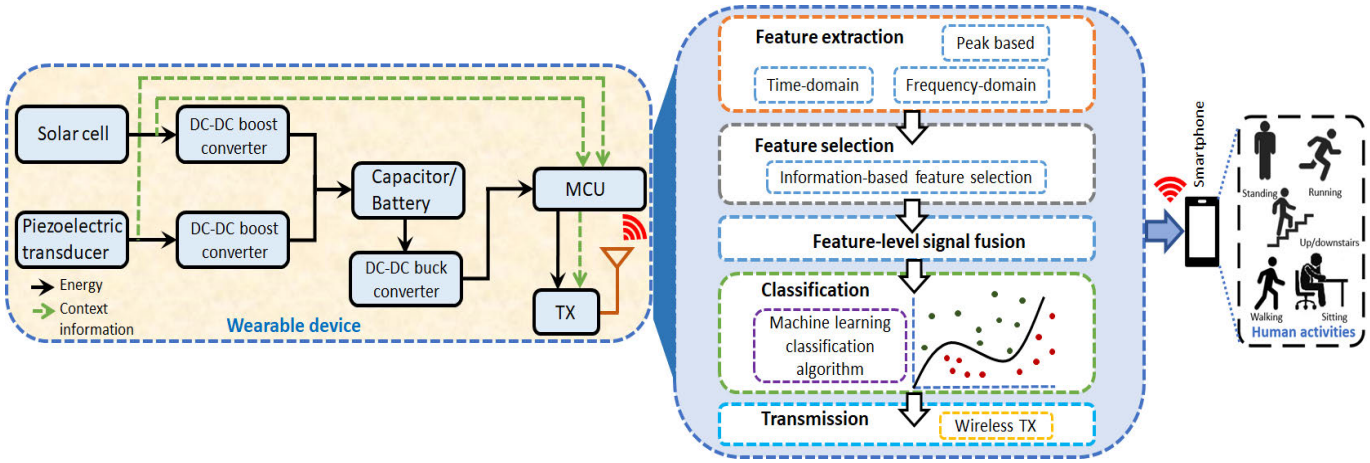

Fig. 3. Proposed FusedAR architecture using the kinetic and solar energy harvesters as activity sensors as well as energy sources simultaneously.

We extract various time- and frequency-domain features from the collected KEH and SEH signals [8], [14]. Later, the most informative features from both energy harvesting signals are selected using well-known feature selection techniques. These selected features are then fused together to combine the context information from both distinct sources to obtain enhanced activity recognition performance. Then, the resultant most dominant features from the fused signal are used to train the classifier. Finally, the inferred activity is transmitted to a nearby receiver where it is used by health, activity, or fitness monitoring applications. In the proposed work, the complete HAR pipeline is implemented on the IoT sensor node, which minimizes the power consumption [32], [33] while simultaneously improving application latency and privacy [34], [35].

B. Measurement Setup

We use Shepherd [36], a portable test bed for the batteryless IoT, which allows recording energy harvesting traces with high resolution, to sample the SEH current signals from a tiny solar cell. This work employs an off-the-shelf IXYS SLMD121H10L solar module for collecting energy harvesting signal during various human activities. The solar cell measures 4.2 × 3.5 cm and weighs 4.5 g, which is appropriate for wearable devices and smart watches [5]. In addition to the solar cell, we simultaneously collect the harvesting current signal from a 7.1- × 2.54-cm MIDÉ technology S230-J1FR-1808XB two-layered piezoelectric bending KEH transducer with a tip mass of 24.62 g ± 0.5% as described in [15] in detail. We use a tip mass to tune the resonance frequency of the KEH (piezoelectric) transducer to the low-frequency vibrations typically observed in human-centric applications [8], resulting in a total mass of 30.46 g. In order to compare our results with the state of the art, we also collect data from a three-axis accelerometer (InvenSense MPU9250). As depicted in Fig. 4, mimicking a wearable device, we place the solar cell, the KEH transducer, and the accelerometer modules on the wrist to record movement during various human activities. Whereas, the recording devices are placed on the waist of the participants, as shown in Fig. 4.

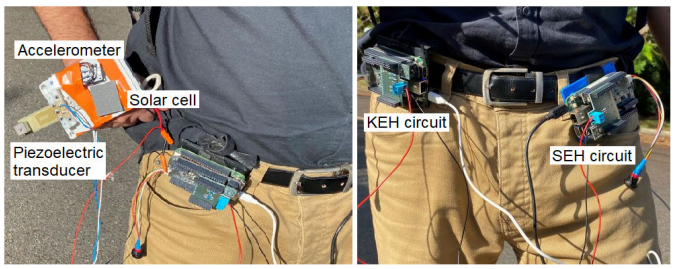

Fig. 4. Data collection setup using SEH and KEH transducers during different daily human activities.

TABLE III
DETAIL OF DATA COLLECTION EXPERIMENTS IN INDOORS AND OUTDOORS

Environment	No. of users	Light source	Surface type	Day/ night
Indoors	9	LED lights	Carpeted room	Day
	4	LED lights	Carpeted room	Night
	5	Fluorescent lights	Tiled hallway	Day
Outdoors	8	Sunlight	Public street	Day
	9	Sunlight	Private street	Day
	5	Street lights	Public street	Night

C. Data Collection

We perform real-world experiments to record SEH, KEH, and three-axis accelerometer data[1] from five common daily human activities, including sitting, standing, walking, running, and going up/downstairs. Table III elaborates that activity data are collected in two different environments, i.e., indoors, and outdoors. The first set of experiments is conducted indoors in various lighting conditions (i.e., LED, and fluorescent lights) with 18 healthy adults (age: 35 ± 10.3 years and mass: 79.7 ± 13.6 kg), and the second set of experiments is performed outdoors (under sunlight and streetlights) with 22 healthy adults

[1]Ethical approval has been granted from CSIRO [106/19] for carrying out this experiment.

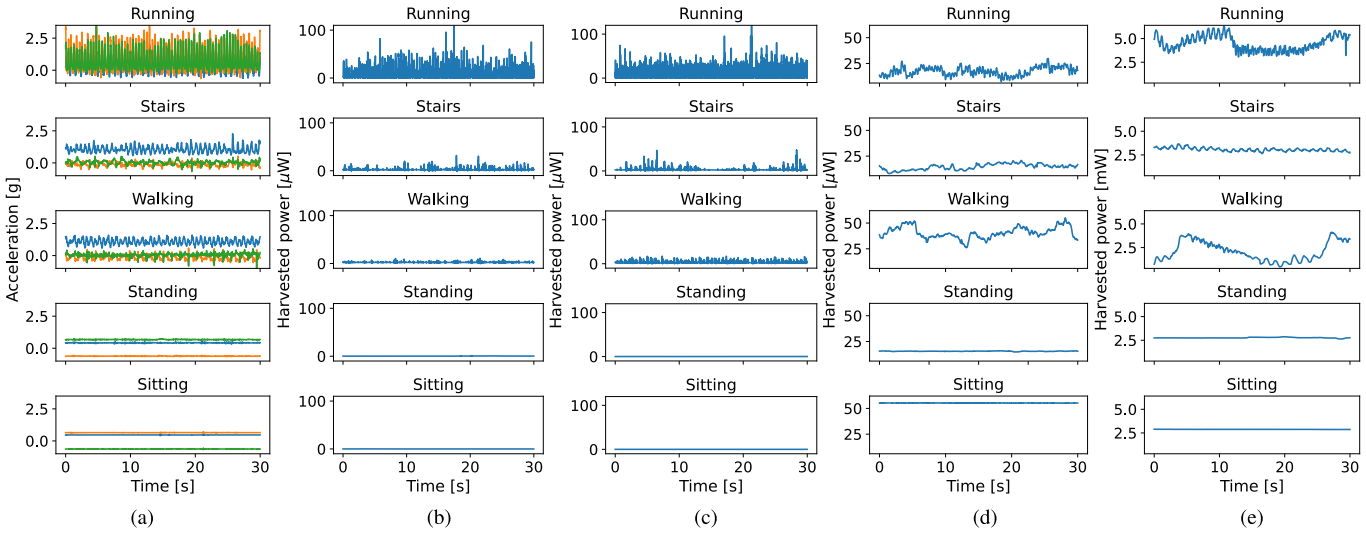

Fig. 5. Wrist-wearable energy harvester/sensor generates distinct pattern of signals during various human activities using (a) three-axis accelerometer, (b) KEH indoors, (c) KEH outdoors, (d) SEH indoors, and (e) SEH outdoors.

(age: 34.2 ± 6.8 years and mass: 78.3 ± 9.6 kg). These volunteers include students and employees of CSIRO working in Brisbane, Australia. In this study, volunteers having different age, mass, and gender are employed to collect representative data of general population performing various activities. In order to collect a representative energy harvesting dataset, which reflects diverse light intensity conditions, we conduct a series of experiments at different locations on different times/days (i.e., morning, noon, evening, and night) with different weather conditions (i.e., sunny, cloudy, and partially cloudy). The participants are advised to perform the activities according to their daily routine and as naturally as possible. Overall, around 600 min of data is recorded from 40 volunteers performing five common human activities. After obtaining the necessary approvals from ethics committee, CSIRO, and the University of Queensland, the anonymized data will be publicly available for the community to promote research in energy harvesting-based HAR.

The sample data traces collected from a wrist-wearable solar cell, a KEH transducer, and a conventional three-axis accelerometer sensor during various human activities are presented in Fig. 5. It shows distinct SEH patterns with unique variations during various human activities in indoor and outdoor environments. It is interesting to notice that the SEH power does not show significant variation during sitting and standing activities due to the lower mobility compared with other dynamic activities. Furthermore, the amount of harvested power is significantly different during sitting and standing activities indoors. It is due to the different orientation and shadowing of the wearable solar cell relative to the indoor light source (resulting in different light intensities) compared with outdoors where light intensity is mostly uniform in daylight conditions. In addition to SEH, we plot the KEH signals from various human activities in Fig. 5. It depicts that the KEH and SEH patterns are distinct not only for various activities but also for different environments (i.e., indoors and outdoors). As a result, the output KEH and SEH signals can be employed to not only distinguish the underlying activities but also the environments in which the activities are performed. To compare our collected signals with the state of the art, we also present three-axis accelerometer traces in Fig. 5, which clearly show unique patterns during various activities.

D. Human Activity Recognition

In the following, we describe the implementation of FusedAR in detail.

1) Preprocessing: The collected data from KEH, SEH, and accelerometer have stop periods between various activities performed by the participants. As these stop periods do not contain useful information about the activity [8], they are removed from the collected data. After removing stop periods, the acquired data are segmented into equal sized 2-s segments [37], which is a typical time duration required to cover one stride length during walking [38]. We also overlap the consecutive data windows before feature extraction to retain the context information at both edges of windows and to increase the number of data points [8]. When we examine the influence of different degrees of window overlap on HAR accuracy, we find that HAR accuracy improves as the degree of window overlap increases. However, increasing the window overlap also increases the latency, complexity, and energy consumption, which is especially important when working with a limited energy budget on resource-constrained embedded devices. Consequently, in accordance with previous works [8], [14], and as a trade-off between energy usage (and latency) and HAR accuracy, we use a window overlap of 50% in this study.

2) Feature Extraction: First, various time-domain, frequency-domain, and peak-based features [8], [14] are extracted from the energy harvesting data (both SEH and KEH signals), as shown in Table IV. Then, to get the smallest set of features that provides the best HAR accuracy, we employ various well-known feature selection algorithms, such as mutual information [39], principal component analysis [40], univariate [41], and correlation-based feature

TABLE IV
SEH SIGNAL FEATURES IN INDOORS AND OUTDOORS

Signal	Features
SEH-indoors	Root-mean-square value, Absolute area, Peak-to-peak value, Coefficient-of-variation, Frequency domain entropy, Max. distance between peaks, Median, Range, 1st Quartile, 2nd Quartile, Spectral peak, Min. value, Max. value, Absolute mean, Mean distance between peaks, Dominant frequency ratio, Kurtosis.
SEH-outdoors	Mean, Absolute area, Peak-to-peak value, Median, Range, Coefficient-of-variation, Frequency domain entropy, Max. distance between peaks, 1st Quartile, 2nd Quartile, 3rd Quartile, Standard deviation, Spectral peak, Min. value, Max. value, Min. peaks, Max. peak, Mean distance between peaks, Median absolute deviation, Frequency domain energy, Autocorrelation.

TABLE V
SELECTED FEATURES FROM THE FUSED SIGNAL IN INDOORS AND OUTDOORS

Signal	Features
Fused-indoors	**SEH:** Max. distance between peaks, Number of peaks, Coefficient-of-variation, Range, Absolute area. **KEH:** Peak-to-peak value, Number of peaks, Absolute area.
Fused-outdoors	**SEH:** Minimum peak value, Max. distance between peaks, Coefficient-of-variation, Minimum value. **KEH:** Absolute area, Peak-to-peak value, Minimum peak value, 3rd quartile, RMS value, Peak value, Number of peaks, Coefficient-of-variation.

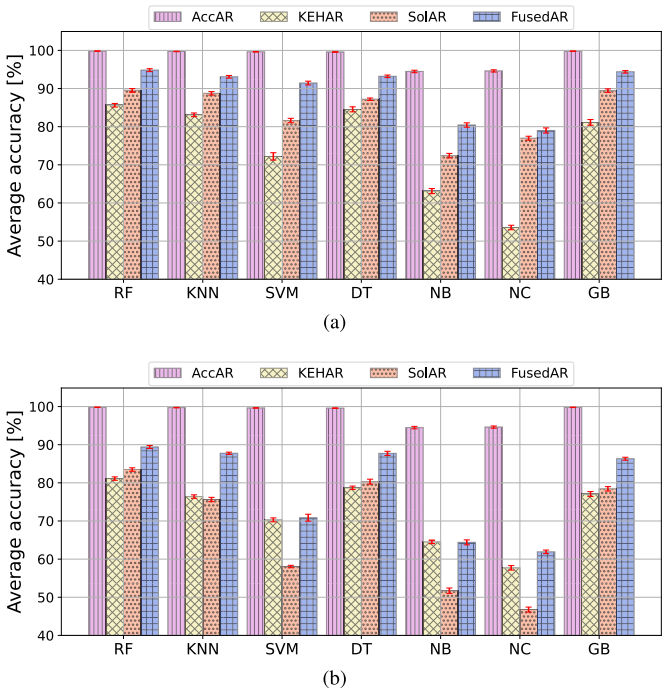

Fig. 6. Average accuracy of AccAR, KEHAR, SolAR, and FusedAR in (a) indoors and (b) outdoors using various classification algorithms (sampling frequency = 100 Hz and window size = 2 s).

selection [42]. After detailed analysis, we discover that the mutual information-based feature selection scheme offers best performance for this dataset, with the smallest number of features as presented in Table IV. It shows that SEH offers 17 and 21 features, and KEH offers 25 and 13 features, in indoor and outdoor settings, respectively. On the other hand, as shown in Table V, FusedAR provides activity information using a significantly reduced feature set, which contains only 8 to 12 features depending on the environment. The advantage of having a reduced feature set is in low energy consumption in processing the collected data on the embedded device and, thus, enhanced active lifetime of IoT sensor nodes.

3) Signal Fusion: In FusedAR, we explore the potential of integrating the high-fidelity context information content present in both KEH and SEH signals to enhance the overall activity recognition performance. In this work, we perform feature-level fusion where we identify the most informative features from the combined KEH and SEH signals using mutual information [39] and present the selected features in Table V. It shows that the fused-indoor signal offers more features from the SEH signal compared with KEH signal due to the increased capability of SEH signal to correctly identify the underlying activities, as depicted in Fig. 6(a). It is also worth noting that inferring the activity from the fused-outdoor signal requires more features from the KEH signal (compared with SEH) to accommodate for the shadowing and interference from the surroundings, which may affect the quality of SEH signal in outdoor environments. Comparing Tables IV and V, we observe that the FusedAR provides detailed activity information using a smaller feature set (i.e., 8–12) compared with using only SolAR (i.e., 17–21 features) and, thus, requires reduced energy (and low latency) in executing the task of feature extraction on the sensor node, as elaborated in Section V-B.

4) Activity Classification and Transmission: Before training a classification algorithm using the collected data, Borderline-synthetic minority oversampling technique (SMOTE) [43] is used to augment the data (from minority class) and handle imbalanced data from various human activities. Later, we implement seven widely used supervised machine learning classifiers, including random forest (RF), decision tree (DT), K-nearest neighbor (KNN), support vector machine (SVM), nearest centroid (NC), Naive Bayes (NB), and gradient boosting (GB), on the collected energy harvesting datasets. The intuition behind using these machine learning models is that they are widely exploited in the literature for low power and online activity recognition applications [44], [45], [46]. Furthermore, as our contribution is to present a better activity recognition signal (using FusedAR) instead of a better classifier, these models are chosen to have a fair comparison between conventional HAR mechanisms and the proposed FusedAR. First, these classification algorithms are trained offline and then imported to the embedded IoT device (this work uses nRF52840) for real-time activity recognition. The result of the output activity is then wirelessly transmitted using Bluetooth low energy (BLE) protocol. Thus, our work not only captures the context/activity signals [14] but also implements

the classification algorithm and end-to-end HAR pipeline on the sensor node using the acquired energy signals, eliminating the requirement for an external energy source. We perform extensive evaluation of FusedAR and SolAR with extended datasets and present the detailed results and insights in the following section.

IV. Performance Evaluation

FusedAR relies on the ambient light and the motion/vibration to generate energy and uses the fused energy harvesting signal for activity recognition. Because the ambient light in indoor and outdoor environments changes significantly, we initially evaluate the performance of FusedAR and SolAR using the data separately from indoor and outdoor experiments, with an extensive comparison with conventional AccAR [46] and KEHAR [8], [14] mechanisms. We next accumulate the data and examine the performance of FusedAR and SolAR in environment-agnostic and environment-preserving scenarios in Section IV-F. All of the results in this research were achieved offline using tenfold cross validation (CV) to allow for comparison with the state of the art (except Section IV-D, which describes the results using leave-one-user-out CV), and are reported with 95% confidence level. The folds are chosen at random from the supplied data to ensure the classifier's robust performance. Prior to implementing the classification algorithms, we augment the collected data from diverse human activities and normalize the features. If not mentioned otherwise, all of the results in this article are acquired using 100-Hz activity signals.

A. Classification Accuracy

Fig. 6 contains the results in terms of HAR accuracy offered by FusedAR and SolAR compared with conventional AccAR [46] and recently proposed KEHAR [8], [14] using various classification algorithms in indoor [see Fig. 6(a)] and outdoor [see Fig. 6(b)] environments. The RF classifier, out of all the classification algorithms, has the highest accuracy for all HAR mechanisms. As a result, the RF classification technique is used to obtain all of the results in the rest of this article. Furthermore, due to the extensive context information encoded in its three-axis accelerometer signal, AccAR [46] provides the best accuracy (more than 99% for all five activities) among the considered mechanisms. For the two individual energy harvesting-based sensing mechanisms, SolAR offers higher accuracy than KEHAR in both indoor and outdoor environments, and SolAR indoors offer higher accuracy than SolAR outdoors. The advantage of SolAR indoors over SolAR outdoors is due to the uniform light exposedness, lower shadowing effect, and the availability of more light sources, which complement each other in indoor environment. On average, SolAR offers up to 4% higher accuracy than KEHAR and at least 10.2% lower accuracy than AccAR for a window size of 2 s. Fig. 6 also presents the average HAR accuracy of FusedAR compared with individual energy harvesting mechanisms (KEHAR and SolAR) and conventional AccAR. It demonstrates that the FusedAR offers significantly higher HAR accuracy compared with SolAR and

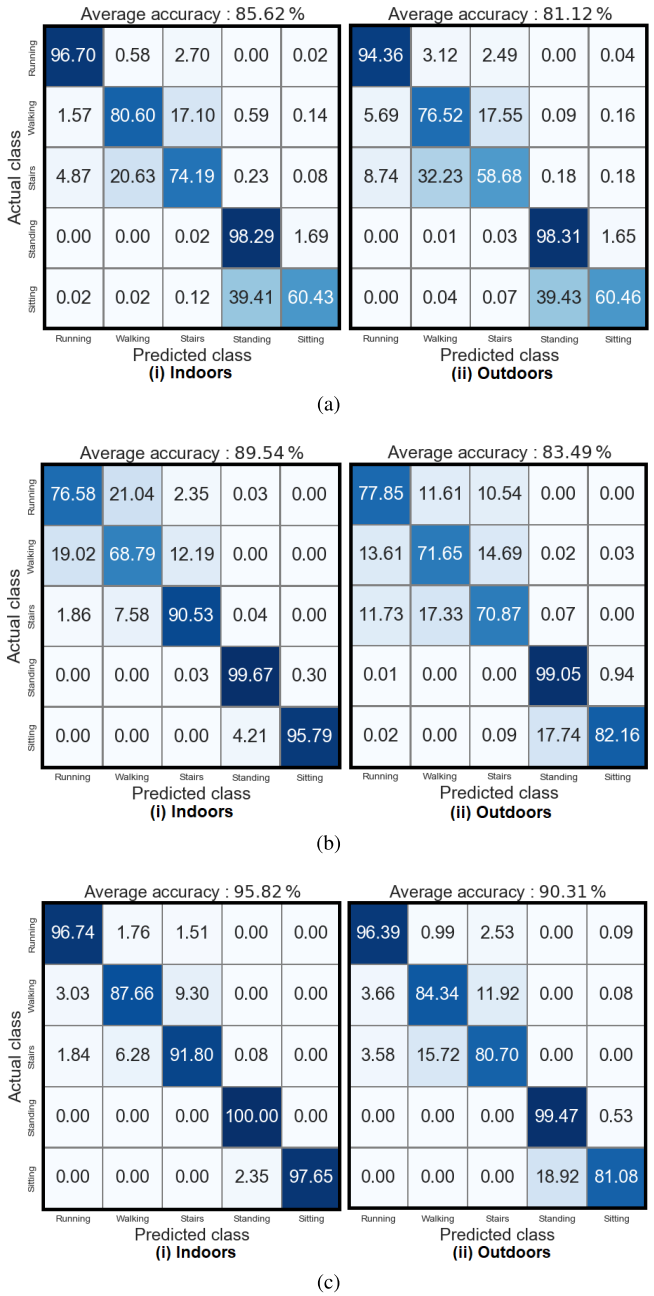

Fig. 7. Confusion matrices using (a) KEHAR, (b) SolAR, and (c) FusedAR in indoors and outdoors (sampling frequency = 100 Hz, window size = 2 s, and RF classifier).

KEHAR in both indoor and outdoor environments and further reduces the accuracy gap to conventional AccAR. This is due to the accumulated rich context information present in the fused signal compared to individual energy harvesting signals, which leads toward enhanced activity recognition performance.

To get more insights on the performance of FusedAR and SolAR compared with KEHAR, we present the confusion matrices for FusedAR, SolAR, and KEHAR in Fig. 7. The confusion matrix of conventional AccAR is not presented, since it offers HAR accuracy of more than 99% in detecting all five activities, as depicted in Fig. 6.

Fig. 7 depicts that outdoor scenarios for both SolAR and KEHAR offer lower HAR accuracy than indoors, in particular

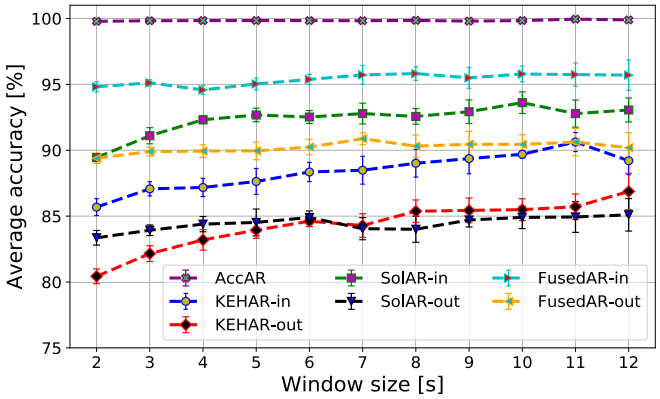

Fig. 8. Average accuracy of AccAR, KEHAR, SolAR, and FusedAR with increasing window sizes in indoors and outdoors (sampling frequency = 100 Hz and RF classifier).

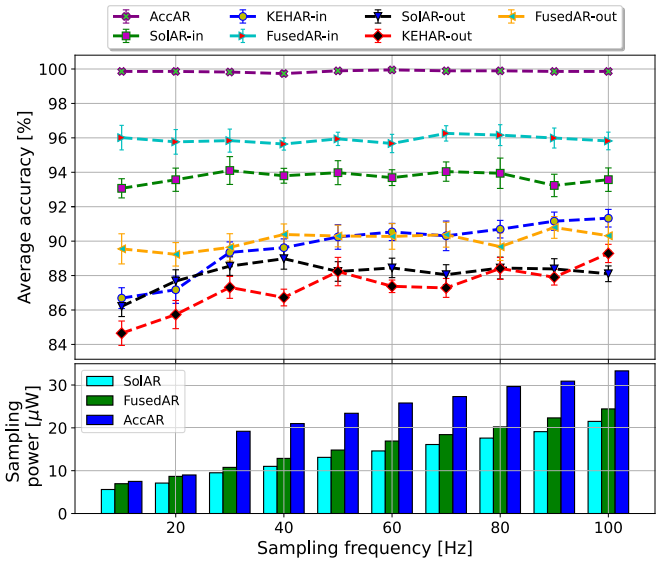

Fig. 9. Average accuracy and required sampling power with varying sampling frequencies of AccAR, KEHAR, SolAR, and FusedAR in indoors and outdoors (window size = 8 s and RF classifier).

during the stairs activity, which can be due to more shadowing and uneven outdoor surface, respectively. We notice that SolAR offers significantly higher HAR accuracy than KEHAR for sitting and stairs activities. This is due to the distinct orientation of SEH transducer relative to the light source that helps SolAR to accurately distinguish sitting from standing and stairs from walking. Whereas, KEHAR struggles to distinguish these activities, which are very similar in their physical motion. In contrast, during walking and running activities, SolAR offers lower accuracy compared with KEHAR. It is due to potentially similar orientation of the solar cell in these activities compared with the significantly distinct movement pattern, which helps KEHAR to take advantage over SolAR in distinguishing those two mobile activities.

FusedAR employs signal fusion using both SEH and KEH signals to take advantage of both energy harvesting signals and enhance the performance closer to the conventional AccAR. The confusion matrices in Fig. 7(c) depict that the fused signal offers improved results for all activities compared with KEHAR and SolAR in both indoor and outdoor environments. This is because the fused signal extracts context information from both energy harvesting signals, which encompasses rich activity information in different dimensions, i.e., changing ambient light and vibrations due to mobility. Thus, both activity signals may complement each other in the fused signal and offer up to 10.2% higher HAR performance compared with individual energy harvesting mechanisms (KEHAR and SolAR) and lower the accuracy gap (only 4.6%) compared with AccAR. In the remaining of Section IV, we further evaluate the performance of SolAR and FusedAR compared with conventional AccAR and KEHAR for varying window sizes, signal sampling frequency, robustness to user variance, robustness to diverse lighting conditions, and environment-agnostic scenarios.

B. Varying Window Sizes

Fig. 8 compares the HAR accuracy of FusedAR, SolAR, KEHAR, and AccAR when varying the window size from 2 to 12 s. As AccAR offers similar performance in both indoor and outdoor environments (see Fig. 6), we plot results only for the indoor scenario in the rest of this article. Fig. 8 shows that AccAR offers a stable accuracy regardless of the window size due to the detailed activity information embedded in its three-axis signal even for smaller window sizes. On the other hand, the accuracy of KEHAR and SolAR (both indoors and outdoors) improves when increasing the window size from 2 to 12 s, which means the window size is an important factor to consider for both KEHAR and SolAR. Fig. 8 also confirms the improved accuracy of FusedAR over individual energy harvesting mechanisms (both indoors and outdoors), which bridges the accuracy gap to AccAR. It is also evident from the figure that FusedAR (both indoors and outdoors) offers a relatively stable accuracy regardless of the window size, which is a similar behavior to AccAR.

It is important to note that increasing the window size results in increased computational complexity, latency, and memory requirements. As a result, the window size should be chosen with the required HAR accuracy, system responsiveness, and processing complexity in mind due to the miniaturized and resource restricted wearable as our target device. Based on the previous explanation, we can see in Fig. 8 that 8 s is the smallest window size that provides the best HAR accuracy for all types of activity signals. As a result, the remaining of the results in this document is provided with an 8-s window.

C. Varying Sampling Frequency of the Signal

Fig. 9 compares the HAR accuracy of FusedAR, SolAR, KEHAR, and AccAR when varying the sampling frequency of the activity signals from 10 to 100 Hz. It also presents the power consumption for sampling the activity signals in FusedAR, SolAR, and AccAR using our measurement setup presented in Section V-B. Fig. 9 depicts that AccAR provides a stable HAR accuracy regardless of the sampling frequency due to the rich activity information present in its three-axis activity signal. On the other hand, KEHAR (both indoors

TABLE VI
AVERAGE ACCURACY FROM THE USER ROBUSTNESS EXPERIMENT (SAMPLING FREQUENCY = 100 Hz, WINDOW SIZE = 8 s, AND RF CLASSIFIER)

Environment	HAR mechanism	10-fold CV	Leave-one-user-out CV
Indoors	KEHAR	91.33	68.89
	SolAR	93.57	83.48
	FusedAR	95.82	91.30
Outdoors	KEHAR	89.28	69.40
	SolAR	88.10	62.53
	FusedAR	90.31	72.89
Overall	AccAR	99.85	90.35

and outdoor) shows an increase in HAR accuracy when varying the sampling rate similar to SolAR outdoors with an increment of about 4% when increasing the sampling rate from 10 to 100 Hz. In contrast, SolAR indoors offer a stable accuracy with very small variation when increasing the sampling rate. It is also evident from Fig. 9 that FusedAR (both indoors and outdoors) offers higher HAR accuracy than individual energy harvesting-based mechanisms (i.e., SolAR and KEHAR) over various sampling frequencies and offers a stable performance when varying the sampling frequency.

The higher sampling rate improves HAR accuracy, because the activity signal has a higher resolution and can capture more fine-grained characteristics of the activity pattern. However, as seen in Fig. 9, energy consumption goes up as sampling frequency rises, owing to the collection of more samples in a given time interval. Fig. 9 shows that FusedAR and SolAR requires up to 27% and 36% lower power than AccAR, respectively, in sampling the activity signal, saving the sensor-related power consumption [8]. In addition, keeping in mind the type of application and the available energy budget, the sampling rate in SolAR and FusedAR can be set as low as 10 Hz to save energy while maintaining activity detection accuracy of over 93% and 96%, respectively.

D. Robustness to User Variance

The robustness of the FusedAR, SolAR, and KEHAR mechanisms against new/unknown users is examined in this section. To this purpose, we employ the RF algorithm, perform a leave-one-user-out CV, and report the averaged findings in Table VI. It shows that FusedAR indoor is the least sensitive to user variation and offers only 4.5% lower average HAR accuracy for unseen users. Furthermore, SolAR indoors and AccAR are slightly more sensitive to the variation in the user and offer 9%–10% lower average accuracy for the unseen users. On the contrary, SolAR outdoors, FusedAR outdoors, and KEHAR indoors/outdoors are significantly affected by the user variance and offer significantly lower average accuracy (17%–25.6%) for new users. This is due to the significant variation in the kinetic harvested energy patterns from different users as well as the more shadowing and interference from the outdoor environment, which affects SolAR outdoors. We expect that a larger training sample from diverse users will further improve the accuracy of the different HAR mechanisms.

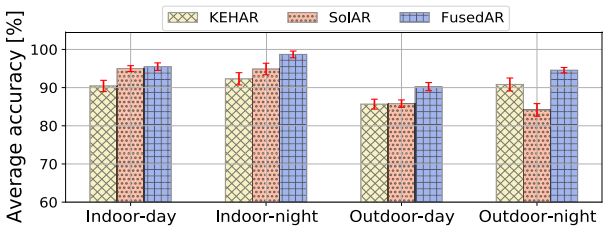

Fig. 10. Average accuracy of KEHAR, SolAR, and FusedAR in diverse lighting conditions (see Table III) in indoors and outdoors (sampling frequency = 100 Hz, window size = 8 s, and RF classifier).

E. Robustness to Diverse Lighting Conditions

As indicated in Table III, we collected energy harvesting data under diverse conditions during day and night in indoor and outdoor environments. In order to explore the performance of FusedAR and SolAR in different lighting conditions, we trained and evaluated these HAR algorithms using individual as well as combined datasets from day and night, as listed in Table III. Fig. 10 shows that SolAR performs 2%–4% better than KEHAR indoors during both day and night due to high-fidelity SEH signal, which captures detailed activity information. In outdoor environment, due to shadowing, SolAR offers similar HAR accuracy as that of KEHAR during daylight, as depicted in Fig. 10. KEHAR offers about 6.7% higher HAR accuracy than SolAR during night time due to insufficient ambient light to embed the activity signature in the harvested solar power to accurately recognize the underlying activities. Finally, Fig. 10 depicts that FusedAR offers higher HAR accuracy than SolAR and KEHAR in various environments (indoors and outdoors) due to the integrated embedded information present in the fused signal as discussed in Section IV-A.

F. Robustness to Environment-Agnostic and Environment-Preserving Scenarios

All of the previous results are obtained using the data collected from indoor and outdoor environments separately. This section explores the performance of FusedAR and SolAR compared with KEHAR when combined data from indoor and outdoor environments are employed. For this analysis, we consider the following two scenarios.

1) *Environment Agnostic:* In this scenario, the data from indoor and outdoor experiments are combined without information about the environment (e.g., walking indoors and walking outdoors are combined as one walking activity).
2) *Environment Preserving:* In this scenario, the data from indoor and outdoor experiments are combined while preserving the condition of the environment (e.g., walking indoors, walking outdoors, running indoors, running outdoors, and so on).

Fig. 11 shows that, in environment-agnostic scenario, KEHAR, SolAR, and FusedAR offer comparable performance

TABLE VII
AVERAGE HARVESTED POWER DURING VARIOUS HUMAN ACTIVITIES USING KEHAR, SOLAR, AND FUSEDAR IN INDOORS AND OUTDOORS

Human activity	Harvested Power [μW]					
	Outdoors			Indoors		
	KEHAR	SolAR	FusedAR	KEHAR	SolAR	FusedAR
Running	9.71	2839	2848.71	6.83	31.88	38.71
Walking	3.14	2263	2266.14	2.50	31.53	34.03
Using stairs	3.63	1802	1805.63	2.77	11.38	14.15
Standing	0.43	867	867.43	0.49	24.54	25.03
Sitting	0.47	1360	1360.47	0.31	49.92	50.23
Average power	**3.48**	**1826**	**1829.48**	**2.60**	**29.85**	**32.45**
Power density [μW/cm^2]	**0.20**	**130.44**	**130.64**	**0.15**	**2.13**	**2.28**

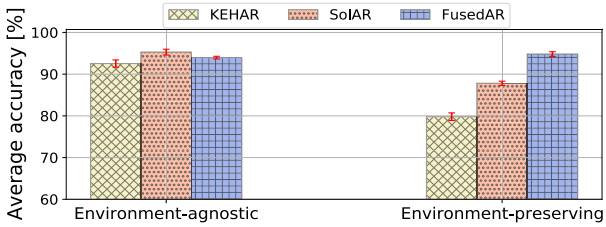

Fig. 11. Average accuracy of KEHAR, SolAR, and FusedAR in environment-agnostic and environment-preserving scenarios (sampling frequency = 100 Hz, window size = 8 s, and RF classifier).

with a small difference of 1.5%–3%. This can be due to the higher incongruity in the solar harvesting signal in indoor and outdoor environments, which may affect the performance of both SolAR and FusedAR, bringing it closer to that of KEHAR. Fig. 11 also shows that, in environment-preserving scenario, SolAR offers 87.8% HAR accuracy in contrast to its counterpart KEHAR, which faces difficulty in recognizing contexts and offers a lower accuracy of 79.8%. This reveals an advantage of SolAR compared with its counterpart KEHAR, which lacks rich information about the contexts in which activities are performed. Fig. 11 also shows that, due to the fusion of both SEH and KEH signals, FusedAR offers higher accuracy (94.8%) than SolAR and KEHAR in environment-preserving scenario. Thus, SolAR and FusedAR can recognize not only human activities but also environment (also called context, such as indoors and outdoors) in which the activities are performed, in contrast to KEHAR, which relies only on vibration/stress of physical human movements.

V. ANALYSIS OF HARVESTED AND CONSUMED POWER

This section analyses the harvested power from SEH and KEH during various human activities as well as the consumed power in implementing the end-to-end HAR algorithm. We find that SolAR and FusedAR offer *energy-positive* HAR as the harvested power exceeds the required power for running the end-to-end HAR algorithm by more than one order of magnitude indoors and two orders of magnitude outdoors.

A. Harvested Power

Using the tool from [36], we sample both voltage and current signals from the energy harvesting transducers, and then compute the average harvested power over a time interval τ as follows:

$$\text{Harvested\_power} = \frac{1}{\tau}\sum_{t=1}^{\tau} \text{voltage}(t) \times \text{current}(t). \quad (1)$$

Table VII presents the average harvested power from KEHAR, SolAR, and FusedAR for the considered human activities in both indoor and outdoor environments. The power density, or harvested power per area, is described in the last row of Table VII. SolAR harvests more than one order of magnitude higher power indoors and more than two orders of magnitude higher power outdoors than KEHAR, due to the higher power density of visible light and superior energy conversion efficiency of solar cells [20]. The results in Table VII also illustrate that the harvested power outdoors are higher than indoors for both SolAR and KEHAR. For solar harvesting, this is because the natural outdoor sunlight has a higher power density compared with the artificial lights indoors. For kinetic harvesting, this can be the result of the following two effects: 1) walking on a paved outside surface produces more vibrations than walking on a carpeted floor indoors [47] and 2) individuals move quicker outdoors, resulting in stronger vibrations and, as a result, higher KEH power. Furthermore, FusedAR offers higher harvested power than SolAR and KEHAR due to the accumulated harvested energy from both transducers.

It is also interesting to note that the harvested power from SolAR is not tightly dependent on the human physical movements compared with KEHAR. Since KEHAR relies on the kinetic energy from the physical movements, it harvests a very small amount of power (0.31–0.49 μW) during static activities, such as standing and sitting. While Shepherd [36] can sample signals with the resolution of 3 μA and 50 μV, the actual amount of harvested power can vary slightly, in particular, during sedentary activities due to significantly lower harvesting voltage and/or current. On the other hand, SolAR can harvest a certain non-zero amount of power during these static activities due to the availability of ambient light. Our experiments show that SolAR generates very small amount of energy at night due to the insignificant light intensity. For example, the average harvested power using SolAR at night is 0.21 μW for running, 0.18 μW for walking, 0.03 μW for

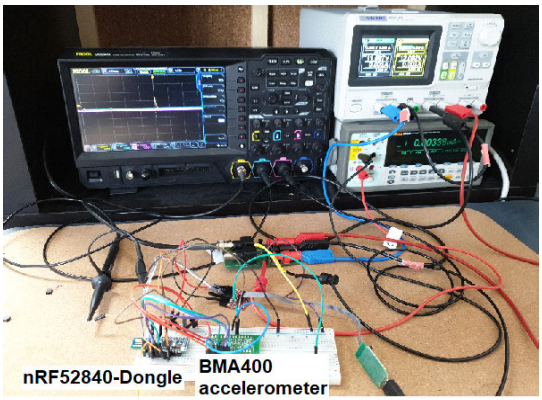

Fig. 12. Experimental setup for measuring the power consumption in sampling the signal and implementing the end-to-end HAR algorithm using AccAR, KEHAR, SolAR, and FusedAR.

using stairs, 0.07 μW for standing, and 0.06 μW for sitting. However, it is worth noting that even with this low level of harvested power during night, SolAR preserves its ability to distinguish the activities using distinct harvested power patterns. Finally, as shown in Table VII, FusedAR provides higher power compared with KEHAR and SolAR due to the accumulation of harvested energy from both transducers. This makes FusedAR most favorable HAR mechanism due to improved performance in both dimensions, i.e., activity recognition and harvested power.

B. Power Consumption

Fig. 12 depicts the hardware setup to measure the power consumption in implementing the complete end-to-end achar algorithm. We use an ultralow power Nordic Semiconductor nRF52840 wireless MCU and a Fluke 8845A multimeter to measure the average current draw. We place a 1-Ω shunt resistor and a TI AD8421 precision amplifier in series with the 3-V supply voltage to measure the dynamic current draw with a Rigol MSO5072 as depicted in Fig. 12. We also use the ultralow power digital accelerometer Bosch BMA400 as a baseline for comparison with state of the art. The firmware is configured to set a dedicated general purpose input–output (GPIO) pin high while performing a task.

The power consumption and execution time of a task can be measured by toggling a GPIO pin and recording the current consumption while the task is being executed. Table VIII compares the average per-task power consumption of running SolAR and FusedAR with KEHAR and AccAR. Based on the results from Section IV, we chose a sampling frequency of 10 Hz and a window size of 8 s, where we extracted the indoor feature set, and use the RF classification algorithm. The result of the inferred activity is then communicated as a BLE packet (periodically after every 8 s), consisting of 6-byte header, 3-byte checksum, and 1-byte payload. Our measurements from Table VIII show that AccAR requires higher power to implement the end-to-end HAR algorithm compared with SolAR and FusedAR mainly due to higher sampling power. Sampling SolAR and FusedAR signals consume 43.45% and 12.41% lower than the power required for sampling the three-axis accelerometer (i.e., 4.35 μW) in AccAR. We also notice slight differences in the average

TABLE VIII
AVERAGE POWER CONSUMPTION WHEN IMPLEMENTING THE END-TO-END HAR ALGORITHM ON THE SENSOR NODE USING ACCAR, KEHAR, SOLAR, AND FUSEDAR IN AN INDOOR ENVIRONMENT (WINDOW SIZE = 8 s)

Task	Average required power [μW]			
	AccAR	KEHAR	SolAR	FusedAR
Sampling (@10 Hz)	4.35	2.46	2.46	3.81
Feature extraction	1.90	2.56	1.64	1.58
Classification	0.05	0.08	0.06	0.07
Data transmission	0.12	0.12	0.12	0.12
Sleep mode	3.15	3.15	3.15	3.15
Total	**9.57**	**8.37**	**7.43**	**8.73**

required power for feature extraction and classification tasks per each mechanism. This is due to the different numbers and types of features to be used as input to the classification algorithm as for each mechanism. Interestingly, the average power consumption of the classifier (0.049–0.089 μW) is one order of magnitude lower than the power required for feature extraction (1.567–2.557 μW) across the board, including AccAR, KEHAR, SolAR, and FusedAR. Overall, the power required to transmit the activity result is 0.125 μW, including 0.067 μW to power up the high frequency clock and 0.058 μW for transmitting the data packet. For the remaining 99.93% of time, the MCU stays in deep sleep mode consuming only 3.15 μW. Thus, as shown in Table VIII, the total average power consumption of our implementation of SolAR and FusedAR is 22.36% and 8.78% lower than the 9.57-μW required power for AccAR, which employs an ultralow power digital three-axis accelerometer as the most efficient state-of-the-art baseline.

It is also worth mentioning that our prototypical implementation is based on discrete off-the-shelf components, and we compare it with the lowest power accelerometers, which have been optimized for decades. For example, the power required for sampling the highly integrated Bosch BMA400 digital accelerometer is two orders of magnitude lower than the power required for sampling an analog accelerometer that is not integrated with the analog-to-digital converter (ADC) (e.g., Analog Devices ADXL356, ~450 μW). By tightly integrating the amplifier with an optimized, low-power ADC, we expect a further reduction of the power consumption in both SolAR and FusedAR in the same order that has been achieved by manufacturers of accelerometers. Moreover, the component cost for our circuit that measures solar current [14], including the amplifier (0.49 USD) and three resistors (<0.01 USD) per device in quantities of 1000, is approximately 0.50 USD. This is lower than a fourth of the price of an ultralow power digital accelerometer (BMA400, 2.16 USD) and lower than a third of the price of the cheapest accelerometer in the same quantity (Kionix Inc. KXTC9-2050-FR, 1.54 USD) that we could find.

C. Energy-Positive HAR

In this part, we compare the harvested power to the power required to run the end-to-end HAR algorithm on the wearable

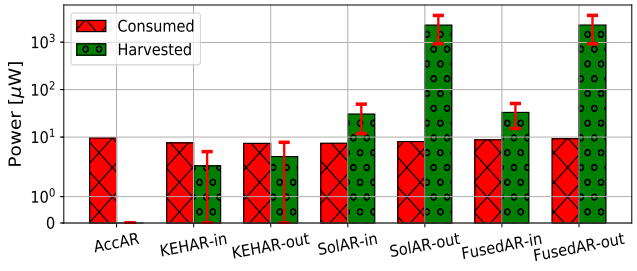

Fig. 13. Average harvested and consumed power in implementing end-to-end HAR algorithm using AccAR, KEHAR, SolAR, and FusedAR in indoors and outdoors.

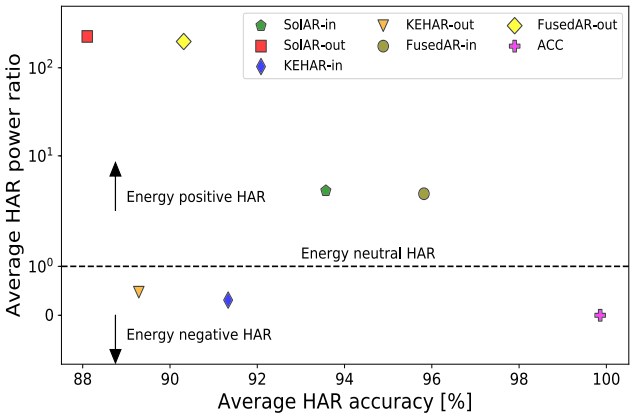

Fig. 14. Average HAR accuracy versus average HAR power ratio using AccAR, KEHAR (KEH size: 18.03 cm^2, 30.46 g), SolAR (SEH size: 14.7 cm^2, 4.5 g), and FusedAR in indoors and outdoors.

device to see if SolAR and FusedAR achieve energy-positive HAR. Therefore, similar to the signal acquisition power ratio in [14], we define the HAR power ratio (P^r_{har}) as follows:

$$P^r_{\text{har}} = \frac{\text{Harvested\_power}}{\text{HAR\_power}}. \tag{2}$$

The system is *energy negative* when the harvested power from a wearable-sized transducer is less than the power required to run the HAR algorithm ($P^r_{\text{har}} < 1$). The system is *energy positive* if the harvested power exceeds the power required to run the HAR algorithm ($P^r_{\text{har}} > 1$). The harvested power from AccAR, KEHAR, SolAR, and FusedAR is compared with the power required to run the HAR algorithm, averaged across all activities in Fig. 13. It shows that the average SolAR harvested power is greater than the power needed to operate the HAR algorithm on the sensor node both indoors and outdoors. SolAR is, thus, *energy positive*, allowing the sensor node to operate autonomously and perpetually without the use of external energy source. Fig. 13 shows that FusedAR also provides higher harvested power (due to high power from SolAR) compared with the required power for running HAR algorithm and, thus, offers *energy-positive* HAR. Despite the fact that the KEH transducer we utilized in our study is larger and heavier than the solar cell (18.03 cm^2, 30.46 g versus 14.7 cm^2, 4.5 g), the average KEH power is insufficient to execute the HAR algorithm on the sensor node, resulting in *energy-negative* HAR. In contrast to SolAR and KEHAR, AccAR does not harvest any power and, thus, offers *energy-negative* HAR according to (2).

We plot the average HAR accuracy and average HAR power ratio using AccAR, KEHAR, SolAR, and FusedAR in Fig. 14. It shows that AccAR and KEHAR indoor/outdoor reside in the *energy-negative* region due to the lower harvested power than the consumed power in implementing the end-to-end HAR algorithm. On the other hand, SolAR and FusedAR offer *energy-positive* HAR in both indoor and outdoor environments due to the higher harvested power compared with the required power in running the HAR algorithm.

VI. Discussion

In contrast to conventional *energy-negative* HAR, which relies on external energy source(s) to power the inertial sensors (such as accelerometers), FusedAR generates sufficient energy to power the wearable IoT device and, thus, offers end-to-end *energy-positive* HAR. This allows uninterrupted and autonomous operation of wearable IoT devices without the need for human intervention. Note that, in contrast to [14], which samples the KEH signal locally and streams the raw data to a server, FusedAR also implements feature extraction, classification, and activity transmission on the wearable device powered only by the harvested energy from the solar panel and KEH transducer. Implementing the complete HAR pipeline on the IoT sensor node not only reduces the power consumption [32], [33], but also improves application latency and privacy [34], [35]. Omitting conventional power-hungry activity sensors, rectification circuits (required for KEHAR), and external energy sources (required for AccAR), FusedAR minimizes the cost, complexity, form factor, and environmental impact of the wearable IoT system. This finally realizes the vision of *energy-positive* HAR, in which end-to-end HAR is performed in real time on the wearable devices using only the harvested energy.

In addition to providing higher energy per area, FusedAR achieves increased HAR accuracy compared with KEHAR and SolAR. Another advantage of FusedAR over KEHAR is that it can recognize not only activities but also the environment/context (i.e., indoors and outdoors), in which activities are performed, while reliably recognizing activities independent of the environment (see Fig. 11). FusedAR can recognize human activities in various lighting conditions and reliably detects the activities even at night time (see Fig. 10) when the ambient light is quite low. Interestingly, FusedAR provides better results on unseen data and offers improved user robustness than KEHAR and SolAR (see Table VI), which proves its applicability in real-world environments. While we considered five strongly dissimilar human activities in this work, we are confident that the proposed algorithm can reliably work in applications that involve even a higher number of activities due to the unique interference and interaction pattern of each activity with the ambient light and generation of distinct vibration patterns. In addition, FusedAR can offer promising results in applications that involve activities in different contexts compared with previous KEH-based HAR. Thus, FusedAR can be employed in applications that demand real-time activity recognition without the need of human

intervention to regularly recharge/replace the batteries of wearable devices.

Although SolAR also provides better results than KEHAR, it needs a light source for its operation, which means that it may face difficulties in recognizing activities in low light conditions, such as at night. In addition, it may not harvest sufficient power at night (and during low light conditions) to allow the perpetual operation of the wearable device. However, these challenges can be addressed by employing FusedAR that provides energy and context information concurrently using KEH and SEH transducers. In order to further enhance the performance, thermal and RF energy harvesters can also be employed in the future to obtain rich context information and higher energy yield.

It is interesting to mention that manually tuned KEH transducers can generate higher power [48] from human movements. However, it is impractical to tune the KEH transducer to specific scenarios. Furthermore, KEH transducers are fundamentally unable to deliver sufficient power during mostly static and sedentary activities. As humans generally spend a great proportion of their time performing such activities (e.g., office work), the average harvested power from KEH transducers may not be adequate to ensure the continuous operation of the wearable sensing devices. Thus, both FusedAR and SolAR offer *energy-positive* HAR for all activities (indoors and outdoors), and the remaining harvested energy can be used to power other body sensors leading toward truly pervasive wearable IoT.

VII. Conclusion and Future Work

This article presents FusedAR, a novel HAR mechanism, which employs miniaturized wearable solar and kinetic energy harvesters for recognizing human activities as well as energy sources. In contrast to conventional accelerometer-based HAR and recently developed KEH-based HAR, FusedAR generates sufficient energy to offer *energy-positive* HAR, in which end-to-end activity recognition algorithm is implemented on the wearable device using only the harvested energy. Rigorous experiments reveal that FusedAR, which combines the respective embedded context information from both solar and kinetic energy harvesters, recognizes not only activities but also the environment/context in which activities are performed (i.e., indoors/outdoors and day/night). As both energy harvesting signals complement each other, the FusedAR offers significantly higher HAR accuracy compared with the individual energy harvesting signals, particularly in nighttime or outdoor environments.

However, this work evaluates FusedAR using only five common human activities. Therefore, in the future, more activities can be included to explore its performance in real environments. Furthermore, in the future, deep learning algorithms can be employed to explore the performance of FusedAR using raw signals. In addition, this work has limitation in terms of implementation of end-to-end HAR classification pipeline on real hardware test beds, which can be investigated in the future.

An interesting future direction is to evaluate FusedAR using an extended activity list and to explore lightweight deep learning models to further enhance the activity recognition accuracy. In addition, studying the practical challenges when running FusedAR online on custom-designed hardware would be an important step toward making energy harvesting-based HAR a reality. Moreover, other energy harvesting sources, such as thermal and RF, can be employed concurrently in the future to provide more energy and context information enhancing the overall performance of the activity recognition system.

Acknowledgment

Muhammad Moid Sandhu was with the School of Information Technology and Electrical Engineering, The University of Queensland, Brisbane, QLD 4072, Australia, and also with Data61 CSIRO, Pullenvale, Brisbane, QLD 4069, Australia. He is now with the Australian e-Health Research Centre, Commonwealth Scientific and Industrial Research Organization (CSIRO), Herston, QLD 4029, Australia (e-mail: moid.sandhu@csiro.au).

Sara Khalifa is with Data61 CSIRO, Pullenvale, Brisbane, QLD 4069, Australia, also with the School of Information Technology and Electrical Engineering, The University of Queensland, Brisbane, QLD 4072, Australia, and also with the School of Computer Science and Engineering, University of New South Wales, Sydney, NSW 2052, Australia (e-mail: sara.khalifa@data61.csiro.au).

Kai Geissdoerfer is with the Networked Embedded Systems Laboratory, Technische Universität (TU) Dresden, 01069 Dresden, Germany (e-mail: kai.geissdoerfer@tu-dresden.de).

Raja Jurdak is with the Trusted Networks Laboratory, School of Computer Science, Queensland University of Technology, Brisbane, QLD 4000, Australia, and also with Data61 CSIRO, Pullenvale, Brisbane, QLD 4069, Australia (e-mail: r.jurdak@qut.edu.au).

Marius Portmann is with the School of Information Technology and Electrical Engineering, The University of Queensland, Brisbane, QLD 4072, Australia (e-mail: marius@itee.uq.edu.au).

Brano Kusy is with Data61 CSIRO, Pullenvale, Brisbane, QLD 4069, Australia (e-mail: brano.kusy@data61.csiro.au).

References

[1] M. Research. (2021). *Wearable Technology Market*. Accessed: Aug. 5, 2021. [Online]. Available: https://www.marketsandmarkets.com/Market-Reports/wearable-electronics-market-983.html

[2] (2021). *Fitbit*. Accessed: Aug. 5, 2021. [Online]. Available: https://www.fitbit.com/au/home

[3] (2021). *Garmin*. Accessed: Aug. 5, 2021. [Online]. Available: https://www.garmin.com/en-AU/

[4] (2021). *Apple Watch*. Accessed: Aug. 5, 2021. [Online]. Available: https://www.apple.com/au/watch/

[5] S. Seneviratne et al., "A survey of wearable devices and challenges," *IEEE Commun. Surveys Tuts.*, vol. 19, no. 4, pp. 2573–2620, 4th Quart., 2017.

[6] Y.-W. Chong, W. Ismail, K. Ko, and C.-Y. Lee, "Energy harvesting for wearable devices: A review," *IEEE Sensors J.*, vol. 19, no. 20, pp. 9047–9062, Oct. 2019.

[7] S. Khalifa, M. Hassan, A. Seneviratne, and S. K. Das, "Energy-harvesting wearables for activity-aware services," *IEEE Internet Comput.*, vol. 19, no. 5, pp. 8–16, Sep. 2015.

[8] S. Khalifa, G. Lan, M. Hassan, A. Seneviratne, and S. K. Das, "HARKE: Human activity recognition from kinetic energy harvesting data in wearable devices," *IEEE Trans. Mobile Comput.*, vol. 17, no. 6, pp. 1353–1368, Jun. 2018.

[9] J. Manjarres, G. Lan, M. Gorlatova, M. Hassan, and M. Pardo, "Deep learning for detecting human activities from piezoelectric-based kinetic energy signals," *IEEE Internet Things J.*, vol. 9, no. 10, pp. 7545–7558, May 2022.

[10] D. Ma et al., "SolarGest: Ubiquitous and battery-free gesture recognition using solar cells," in *Proc. 25th Annu. Int. Conf. Mobile Comput. Netw.*, Aug. 2019, pp. 1–15.

[11] D. Ma et al., "Recognizing hand gestures using solar cells," *IEEE Trans. Mobile Comput.*, early access, Feb. 4, 2022, doi: 10.1109/TMC.2022.3148143.

[12] Y. Umetsu, Y. Nakamura, Y. Arakawa, M. Fujimoto, and H. Suwa, "EHAAS: Energy harvesters as a sensor for place recognition on wearables," in *Proc. IEEE Int. Conf. Pervasive Comput. Commun. (PerCom*, Mar. 2019, pp. 1–10.

[13] G. Lan, D. Ma, W. Xu, M. Hassan, and W. Hu, "Capacitor-based activity sensing for kinetic-powered wearable IoTs," *ACM Trans. Internet Things*, vol. 1, no. 1, pp. 1–26, Feb. 2020.

[14] M. M. Sandhu, K. Geissdoerfer, S. Khalifa, R. Jurdak, M. Portmann, and B. Kusy, "Towards energy positive sensing using kinetic energy harvesters," in *Proc. IEEE Int. Conf. Pervasive Comput. Commun. (PerCom)*, Mar. 2020, pp. 1–10.

[15] M. M. Sandhu, S. Khalifa, K. Geissdoerfer, R. Jurdak, and M. Portmann, "SolAR: Energy positive human activity recognition using solar cells," in *Proc. IEEE Int. Conf. Pervasive Comput. Commun. (PerCom)*, Mar. 2021, pp. 1–10.

[16] A. Bulling, U. Blanke, and B. Schiele, "A tutorial on human activity recognition using body-worn inertial sensors," *ACM Comput. Surv.*, vol. 46, no. 3, pp. 1–33, Jan. 2014.

[17] D. Ma, G. Lan, W. Xu, M. Hassan, and W. Hu, "SEHS: Simultaneous energy harvesting and sensing using piezoelectric energy harvester," in *Proc. IEEE/ACM 3rd Int. Conf. Internet Things Design Implement. (IoTDI)*, Apr. 2018, pp. 201–212.

[18] M. M. Sandhu, K. Geissdoerfer, S. Khalifa, R. Jurdak, M. Portmann, and B. Kusy, "Towards optimal kinetic energy harvesting for the batteryless IoT," in *Proc. IEEE Int. Conf. Pervasive Comput. Commun. Workshops (PerCom Workshops)*, Mar. 2020, pp. 1–6.

[19] B. Pozo, J. I. Garate, J. A. Araujo, and S. Ferreiro, "Energy harvesting technologies and equivalent electronic structural models–review," *Electronics*, vol. 8, no. 5, p. 486, Apr. 2019.

[20] N. A. Bhatti, M. H. Alizai, A. A. Syed, and L. Mottola, "Energy harvesting and wireless transfer in sensor network applications: Concepts and experiences," *ACM Trans. Sensor Netw.*, vol. 12, no. 3, pp. 1–40, Aug. 2016.

[21] F. John Dian, R. Vahidnia, and A. Rahmati, "Wearables and the Internet of Things (IoT), applications, opportunities, and challenges: A survey," *IEEE Access*, vol. 8, pp. 69200–69211, 2020.

[22] B. L. Smarr et al., "Feasibility of continuous fever monitoring using wearable devices," *Sci. Rep.*, vol. 10, no. 1, pp. 1–11, Dec. 2020.

[23] H. C. Ates, A. K. Yetisen, F. Güder, and C. Dincer, "Wearable devices for the detection of COVID-19," *Nature Electron.*, vol. 4, no. 1, pp. 13–14, Jan. 2021.

[24] A. Ramadhan, "Wearable smart system for visually impaired people," *Sensors*, vol. 18, no. 3, p. 843, Mar. 2018.

[25] T. Sztyler, H. Stuckenschmidt, and W. Petrich, "Position-aware activity recognition with wearable devices," *Pervas. Mobile Comput.*, vol. 38, pp. 281–295, Jul. 2017.

[26] G. Lan, D. Ma, W. Xu, M. Hassan, and W. Hu, "CapSense: Capacitor-based activity sensing for kinetic energy harvesting powered wearable devices," in *Proc. 14th EAI Int. Conf. Mobile Ubiquitous Syst., Comput., Netw. Services*, 2018, pp. 106–115.

[27] H. Kalantarian, N. Alshurafa, T. Le, and M. Sarrafzadeh, "Monitoring eating habits using a piezoelectric sensor-based necklace," *Comput. Biol. Med.*, vol. 58, pp. 46–55, Mar. 2015.

[28] G. Lan, W. Xu, D. Ma, S. Khalifa, M. Hassan, and W. Hu, "EnTrans: Leveraging kinetic energy harvesting signal for transportation mode detection," *IEEE Trans. Intell. Transp. Syst.*, vol. 21, no. 7, pp. 2816–2827, Jul. 2020.

[29] Q. Lin et al., "H2B: Heartbeat-based secret key generation using Piezo vibration sensors," in *Proc. 18th Int. Conf. Inf. Process. Sensor Netw.*, Apr. 2019, pp. 265–276.

[30] L. He et al., "A novel self-powered sensor based on $Ni(OH)_2/Fe_2O_3$ photoanode for glucose detection by converting solar energy into electricity," *J. Alloys Compounds*, vol. 907, Jun. 2022, Art. no. 164132.

[31] H. Sharma, A. Haque, and Z. Jaffery, "Modeling and optimisation of a solar energy harvesting system for wireless sensor network nodes," *J. Sensor Actuator Netw.*, vol. 7, no. 3, p. 40, Sep. 2018.

[32] H. Rezaie and M. Ghassemian, "An adaptive algorithm to improve energy efficiency in wearable activity recognition systems," *IEEE Sensors J.*, vol. 17, no. 16, pp. 5315–5323, Aug. 2017.

[33] X. Fafoutis, L. Marchegiani, A. Elsts, J. Pope, R. Piechocki, and I. Craddock, "Extending the battery lifetime of wearable sensors with embedded machine learning," in *Proc. IEEE 4th World Forum Internet Things (WF-IoT)*, Feb. 2018, pp. 269–274.

[34] A. Wang, L. Chen, and W. Xu, "Xpro: A cross-end processing architecture for data analytics in wearables," *ACM SIGARCH Comput. Archit. News*, vol. 45, no. 2, pp. 69–80, 2017.

[35] M. Verhelst and B. Moons, "Embedded deep neural network processing: Algorithmic and processor techniques bring deep learning to IoT and edge devices," *IEEE Solid State Circuits Mag.*, vol. 9, no. 4, pp. 55–65, Fall 2017.

[36] K. Geissdoerfer, M. Chwalisz, and M. Zimmerling, "Shepherd: A portable testbed for the batteryless IoT," in *Proc. 17th Conf. Embedded Netw. Sensor Syst.*, Nov. 2019, pp. 83–95.

[37] A. Stisen et al., "Smart devices are different: Assessing and mitigating-mobile sensing heterogeneities for activity recognition," in *Proc. 13th ACM Conf. Embedded Netw. Sensor Syst.*, Nov. 2015, pp. 127–140.

[38] Y. P. Lim, Y.-C. Lin, and M. G. Pandy, "Effects of step length and step frequency on lower-limb muscle function in human gait," *J. Biomech.*, vol. 57, pp. 1–7, May 2017.

[39] B. C. Ross, "Mutual information between discrete and continuous data sets," *PLoS ONE*, vol. 9, no. 2, Feb. 2014, Art. no. e87357.

[40] T. P. Minka, "Automatic choice of dimensionality for PCA," in *Proc. Adv. Neural Inf. Process. Syst.*, 2001, pp. 598–604.

[41] T. Emura, S. Matsui, and H.-Y. Chen, "Compound.Cox: Univariate feature selection and compound covariate for predicting survival," *Comput. Methods Programs Biomed.*, vol. 168, pp. 21–37, Jan. 2019.

[42] M. Mursalin, Y. Zhang, Y. Chen, and N. V. Chawla, "Automated epileptic seizure detection using improved correlation-based feature selection with random forest classifier," *Neurocomputing*, vol. 241, pp. 204–214, Jun. 2017.

[43] H. Han, W.-Y. Wang, and B.-H. Mao, "Borderline-SMOTE: A new over-sampling method in imbalanced data sets learning," in *Proc. Int. Conf. Intell. Comput.* Cham, Switzerland: Springer, 2005, pp. 878–887.

[44] S. Balli, E. A. Sağbaş, and M. Peker, "Human activity recognition from smart watch sensor data using a hybrid of principal component analysis and random forest algorithm," *Meas. Control*, vol. 52, nos. 1–2, pp. 37–45, Jan. 2019.

[45] G. Bhat, R. Deb, V. V. Chaurasia, H. Shill, and U. Y. Ogras, "Online human activity recognition using low-power wearable devices," in *Proc. IEEE/ACM Int. Conf. Comput.-Aided Design (ICCAD)*. Nov. 2018, pp. 1–8.

[46] T.-H. Dao, H.-Y. Hoang, V.-N. Hoang, D.-T. Tran, and D.-N. Tran, "Human activity recognition system for moderate performance microcontroller using accelerometer data and random forest algorithm," *EAI Endorsed Trans. Ind. Netw. Intell. Syst.*, vol. 9, no. 4, p. e4, Nov. 2022.

[47] H. B. Menz, S. R. Lord, and R. C. Fitzpatrick, "Acceleration patterns of the head and pelvis when walking on level and irregular surfaces," *Gait Posture*, vol. 18, no. 1, pp. 35–46, Aug. 2003.

[48] Y. Kuang, T. Ruan, Z. J. Chew, and M. Zhu, "Energy harvesting during human walking to power a wireless sensor node," *Sens. Actuators A, Phys.*, vol. 254, pp. 69–77, Feb. 2017.

Muhammad Moid Sandhu (Member, IEEE) received the Ph.D. degree from the School of Information Technology and Electrical Engineering, The University of Queensland, Brisbane, QLD, Australia, in 2022, in collaboration with Data61 CSIRO, Pullenvale, Brisbane, QLD, Australia.

He is currently a Postdoctoral Research Fellow with the Australian e-Health Research Centre, Commonwealth Scientific and Industrial Research Organization (CSIRO), Herston, QLD, Australia. He has been working on the design and implementation of smart sensing technologies for human activity, health, and fitness monitoring applications. He has published several research papers in various well-reputed and peer-reviewed international journals and conferences. He has also authored a book *Self-Powered Internet of Things: How Energy Harvesters can Enable Energy-Positive Sensing, Processing, and Communication* in 2023. His research interests include eHealth, digital health, wearables, the IoT, context detection, pervasive computing, and embedded machine learning.

Dr. Sandhu has received the Gold Medal and Academic Roll of Honor for his outstanding performance during his B.Sc. degree in electrical engineering in 2012.

Sara Khalifa (Member, IEEE) received the Ph.D. degree in computer science and engineering from the University of New South Wales (UNSW), Sydney, NSW, Australia, in 2016.

She is currently the Senior Research Scientist of the Distributed Sensing Systems Research Group, Data61 CSIRO, Pullenvale, Brisbane, QLD, Australia. She is also an Honorary Adjunct Lecturer with The University of Queensland, Brisbane, QLD, Australia, and a Conjoint Lecturer with UNSW. Her research interests rotate around the broad aspects of mobile and ubiquitous computing, mobile sensing, and the Internet of Things (IoT).

Dr. Khalifa's Ph.D. dissertation received the 2017 John Makepeace Bennett Award which is awarded by Computing Research and Education Association of Australasia (CORE) to the Best Ph.D. Dissertation of the year within Australia and New Zealand in the field of computer science. Her research has been recognized by multiple iAwards, including the 2017 NSW Mobility Innovation of the year, the 2017 NSW Research and Development Innovation of the year, the National Merit Research and Development Innovation of the year, and the Merit Research and Development Award at the Asia–Pacific ICT Alliance (APICTA) Awards, commonly known as the "Oscar" of the ICT industry in Asia–Pacific, among others.

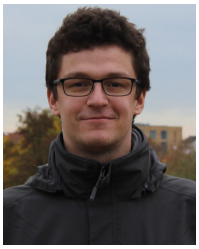

Kai Geissdoerfer received the B.Sc. and M.Sc. degrees in electrical engineering from Technische Universität (TU) Berlin, Berlin, Germany, in 2015 and 2017, respectively, and the Ph.D. degree from the Networked Embedded Systems Laboratory, Technische Universität (TU) Dresden, Dresden, Germany, in 2022.

He is a Postdoctoral Researcher with the Networked Embedded Systems Laboratory, TU Dresden. He has been a Visiting Research Student with the Distributed Sensing Systems Group, Data61 CSIRO, Pullenvale, Brisbane, QLD, Australia, since 2017. His research interests include battery-free, energy harvesting devices.

Raja Jurdak (Senior Member, IEEE) received the B.E. degree in computer and communications engineering from the American University of Beirut, Beirut, Lebanon, in 2000, the M.S. degree in computer networks and distributed computing from the Department of Electrical and Computer Engineering, University of California at Irvine, Irvine, CA, USA, in 2001, and the Ph.D. degree in information and computer science from the University of California at Irvine in 2005.

He is a Professor of Distributed Systems and the Chair in Applied Data Sciences at the Queensland University of Technology, Brisbane, QLD, Australia, where he is also the Director of the Trusted Networks Laboratory. He is also an Adjunct Professor with the University of New South Wales, Sydney, NSW, Australia. He previously established and led the Distributed Sensing Systems Group, Data61 CSIRO, Pullenvale, Brisbane, QLD, Australia. He also spent time as Visiting Academic at MIT, Cambridge, MA, USA, and Oxford University, Oxford, U.K., in 2011 and 2017, respectively. He has published more than 250 peer-reviewed publications, including two authored books most recently on blockchain in cyberphysical systems in 2020. His publications have attracted over 12 500 citations, with an H-index of 49. His research interests include trust, mobility, and energy-efficiency in networks.

Dr. Jurdak serves on the Editorial Board of *Ad Hoc Networks* and *Scientific Reports* (Nature), and on the Organizing and Technical Program Committees of top international conferences, including Percom, IEEE International Conference on Blockchain and Cryptocurrency (ICBC), IEEE/ACM International Conference on Information Processing in Sensor Networks (IPSN), International Symposium on a World of Wireless, Mobile and Multimedia Networks (WoWMoM), and IEEE International Conference on Distributed Computing Systems (ICDCS). He was the TPC Co-Chair of ICBC in 2021. He is a Distinguished Visitor of the IEEE Computer Society.

Marius Portmann (Member, IEEE) received the Ph.D. degree in electrical engineering from the Swiss Federal Institute of Technology (ETH) Zürich, Zürich, Switzerland, in 2002.

He is currently an Associate Professor with The University of Queensland, Brisbane, QLD, Australia. His research interests include general networking, in particular software-defined networking (SDN), wireless networks, pervasive computing, and cyber security.

Brano Kusy (Member, IEEE) received the Ph.D. degree from Vanderbilt University, Nashville, TN, USA, in 2007.

He is the Principal Research Scientist and the Group Leader of the Distributed Sensing Systems, CSIRO, Pullenvale, Brisbane, QLD, Australia. He is also an adjunct Associate Professor with The University of Queensland, Brisbane, QLD, Australia. His research interests include embedded networked systems and algorithms, with a specific focus on in situ sensing and intelligence to allow the IoT systems to respond to real-world challenges in an autonomous way.

Dr. Kusy is an internationally respected Scientist. He has served as the General Chair for IEEE/ACM International Conference on Information Processing in Sensor Networks (IPSN) 2020. He is regularly involved in the Program Committees of top-ranked international conferences ACM Conference on Embedded Networked Sensor Systems (ACM SensSys), ACM/IEEE International Conference on Information Processing in Sensor Networks (IPSN), International Conference on Embedded Wireless Systems and Networks (EWSN), IEEE International Conference on Mobile Ad-Hoc and Smart Systems (MASS), and IEEE International Conference on Distributed Computing Systems (ICDCS). He has served on the TinyOS Core Working Group.